



---

# A Wavelet Transformation based Performance Analysis on Image Denoising

Aarti Gupta<sup>1</sup>, Prof. Jitendra Mishra<sup>2</sup>

<sup>1</sup>M. Tech. Scholar, Department of EC, PCST, Bhopal (India)

<sup>2</sup>Head & Professor, Department of EC, PCST, Bhopal (India)

**Abstract:** *Visual information transmitted in the form of digital images is becoming a major method of communication in the modern age, but the image obtained after transmission is often corrupted with noise. The received image needs processing before it can be used in applications. Image denoising involves the manipulation of the image data to produce a visually high quality image. This process of image denoising is done by using methods that are with like wavelet transformation, wiener filter and mean filter. This all methods implemented in MATLAB. The input images are used here for the measured of image denoising techniques comparative performance used barbara image, cameraman image and house image, here proposed method gives better results than the existing work.*

**Keywords:** Edge detection, Wiener filter, Wavelet transformation, Image denoising, Matlab.

## Introduction

A very large portion of digital image processing is devoted to image restoration. This includes research in algorithm development and routine goal oriented image processing. Image restoration is the removal or reduction of degradations that are incurred while the image is being obtained. Degradation comes from blurring as well as noise due to electronic and photometric sources. Blurring is a form of bandwidth reduction of the image caused by the imperfect image formation process such as relative motion between

the camera and the original scene or by an optical system that is out of focus. When aerial photographs are produced for remote sensing purposes, blurs are introduced by atmospheric turbulence, aberrations in the optical system and relative motion between camera and ground. In addition to these blurring effects, the recorded image is corrupted by noises too. A noise is introduced in the transmission medium due to a noisy channel, errors during the measurement process and during quantization of the data for digital storage. Each element in the imaging chain such as lenses, film, digitizer, etc. contribute to the degradation. Image denoising is often used in the field of photography or publishing where an image was somehow degraded but needs to be improved before it can be printed. For this type of application we need to know something about the degradation process in order to develop a model for it. When we have a model for the degradation process, the inverse process can be applied to the image to restore it back to the original form. This type of image restoration is often used in space exploration to help eliminate artifacts generated by mechanical jitter in a spacecraft or to compensate for distortion in the optical system of a telescope. Image denoising finds applications in fields such as astronomy where the resolution limitations are severe, in medical imaging where the physical requirements for high quality imaging are needed for analyzing images of unique events, and in forensic science where potentially useful photographic evidence is sometimes of



extremely bad quality. Let us now consider the representation of a digital image. A 2-dimensional digital image can be represented as a 2-dimensional array of data  $s(x,y)$ , where  $(x,y)$  represent the pixel location. The pixel value corresponds to the brightness of the image at location  $(x,y)$ . Some of the most frequently used image types are binary, gray-scale and color images. Binary images are the simplest type of images and can take only two discrete values, black and white. Black is represented with the value '0' while white with '1'. Note that a binary image is generally created from a gray-scale image. A binary image finds applications in computer vision areas where the general shape or outline information of the image is needed. They are also referred to as 1 bit/pixel images. Gray-scale images are known as monochrome or one-color images. The images used for experimentation purposes in this thesis are all gray-scale images. They contain no color information. They represent the brightness of the image. This image contains 8 bits/pixel data, which means it can have up to 256 (0-255) different brightness levels. A '0' represents black and '255' denotes white. In between values from 1 to 254 represent the different gray levels. As they contain the intensity information, they are also referred to as intensity images. Color images are considered as three band monochrome images, where each band is of a different color. Each band provides the brightness information of the corresponding spectral band. Typical color images are red, green and blue images and are also referred to as RGB images.

## **II. Digital Image**

Digital media offer several distinct advantages over analog media: the quality of digital audio, images and video signals are higher than that of their analog counterparts. Editing is easy because one can access the exact discrete locations that should be changed. Copying is simple with no loss of fidelity. Additional advantages include: the ease with which they can be displayed on computer monitors, and their appearance modified at will; the ease with which

they can be stored on, for example, CD-ROM or DVD; the ability to send them between computers, via the internet or via satellite; the option to compress them to save on storage space or reduce communication times. Many of these advantages are particularly relevant to medical imaging. Increasingly, hospitals are networking their digital imaging systems into so-called PACS (Picture and Archiving Systems, RIS/HIS (Radiological/Hospital Information Systems), which include patient diagnosis and billing details along with the images. A two dimensional digital image can be represented as a two dimensional array of data  $U(i,j)$ , where  $(i,j)$  represent the pixel location. The pixel value corresponds to the brightness of the image at location  $(i,j)$ . Some of the most frequently used image types are binary, gray-scale and color images. Binary images are the simplest type of images and can take only two discrete values, black and white. Black is represented with the value „0“ while white with „1“. Note that a binary image is generally created from a gray-scale image. A binary image finds applications in computer vision areas where the general shape or outline information of the image is needed. They are also referred to as one bit/pixel images. Gray-scale images are known as monochrome or one-color images. The images used for experimentation purposes in this thesis are all gray-scale images. They contain no color information. They represent the brightness of the image. This image contains eight bits/pixel data, which means it can have up to 256 (0-255) different brightness levels. A '0' represents black and '255' denotes white. In between values from 1 to 254 represent the different gray levels. As they contain the intensity information, they are also referred to as intensity images. Color images are considered as three band monochrome images, where each band is of a different color.

## **III. Proposed Work**

For a wavelet transform, two filters are required – a low-pass filter, which constructs the low frequency component, and a high-pass filter, which constructs the high-frequency component. These filters are



chosen such that the original signal can later be reconstructed from a combination of the low and high frequency components. This is known as an inverse transform and it requires two reconstruction filters – one which reconstructs the even-indexed samples, the other which reconstructs the odd-indexed samples. Perhaps the simplest filter bank is the Haar filter bank. The non-normalized low-pass filter is  $[1, 1]$ , and the non-normalized high-pass filter is  $[1, -1]$  [25]. It can be seen that these filters correspond to the sums and differences of the signal, respectively. To show a worked example, using the signal  $[1, 7, 7, 5, 4, 8, 7, 9]$ , the circular convolution with the low-pass filter gives  $[8, 14, 12, 9, 12, 15, 16, 10]$ , and the circular convolution with the high-pass filter gives  $[-6, 0, 2, 1, -4, 1, -2, 8]$ . As will be shown, all odd-indexed values can be discarded, leaving  $[8, 12, 12, 16]$  and  $[-6, 2, -4, -2]$ . Normalizing these filters by a factor of 0.5 gives the averages and half-differences instead –  $[4, 6, 6, 8]$  for the low frequency and  $[-3, 1, -2, -1]$  for the high frequency signals. It can now be seen that, for a pair of values, if the average and half-difference are saved, then the original pair can be recovered. For the first value of the pair, the average and the half-difference have to be summed, and for the second value, the half-difference has to be subtracted from the average. This gives us the reconstruction filters  $[1, 1]$  and  $[1, -1]$ . It is mostly a coincidence that they coincide with the low and high-pass filters. For this simple example, it can be worked out by hand that using the described procedure indeed gives back the original signal. For longer filters, however, it would be simpler to define this operation as convolution. First, the low and high frequency signals must be interleaved, giving  $[4, -3, 6, 1, 6, -2, 8, -1]$ . This signal is convolved with each filter, and the odd-indexed values are again discarded, leaving  $[1, 7, 4, 7]$  and  $[7, 5, 8, 9]$ . Interleaving these gives back the original signal. The same algorithm can be used for longer filters as well. Another benefit of the DWT is that the resulting low frequency signal resembles the original signal. This means the DWT can be applied to the low frequency component multiple times at different levels, each

time obtaining the high frequency component of that level and an even lower frequency component. The low- and high-pass filters  $H_0$  and  $H_1$  produce higher level low and high frequency representation of the current level low frequency coefficients. Both signals are then downsampled, indicated by the down arrow, removing every other value. The high frequency coefficients of the  $n$ -th decomposition level are saved as  $W_\psi[J - n, k]$ , while the low frequency component can be filtered further. The process can be inverted from the final low and high frequency wavelet coefficients by using the reconstruction filters  $G_0$  and  $G_1$ . The highest level low and high frequency signals are upsampled, indicated by the up arrow, by adding zeroes for every other value, filtered with the corresponding reconstruction filters, then added together to get the one level lower low frequency signal. The process is repeated with the reconstructed signal and the next high frequency signal until the original image is reconstructed. This multi-level decomposition is a useful step because it enables applying different amounts of denoising and compression to different levels. By its nature, noise occurs primarily in the high frequency component, so it makes sense to apply stronger denoising to that component. Further, as images are largely comprised of smooth gradients or flat areas of color with relatively few details such as edges, the low frequency components carry more useful information. For this reason, it is not as harmful to the quality of an image if information is lost from the high frequency components due to denoising or compression in comparison to losing information from the low frequency components.

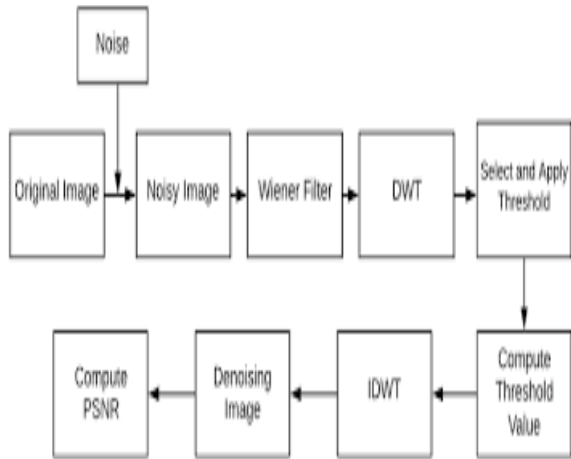


Fig 1: The present work block diagram.

#### IV. Experimental Result

In this section the experimental process of image denoising techniques comparative performance is measured with the performance parameter. This process of image denoising is done by using methods that are with like wavelet transformation, wiener filter and mean filter. This all methods implemented in MATLAB. The input images are used here for the measured of image denoising techniques comparative performance used barbara image, cameraman image and house image etc.

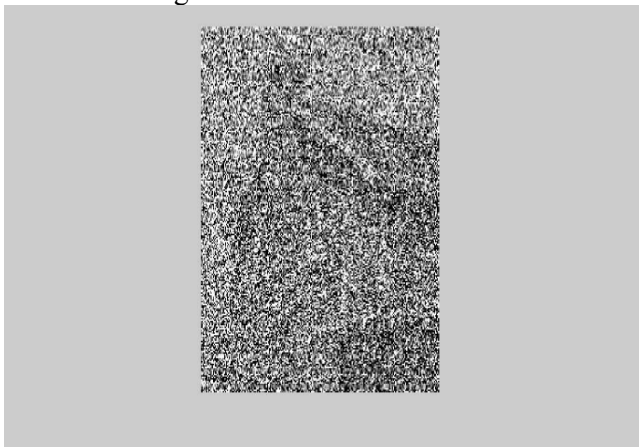


Fig 2: This picture presents the house processing image for experimental work using mean filter technique.

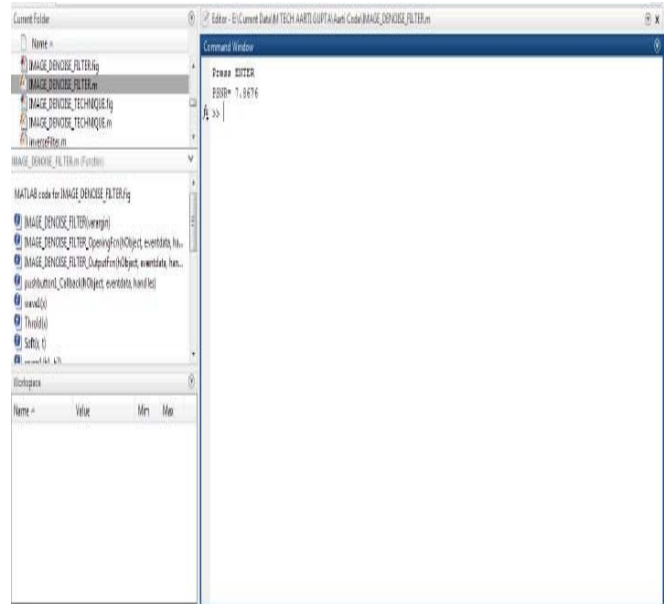


Fig 3: This picture presents the result of house processing image using mean filter technique with PSNR value.

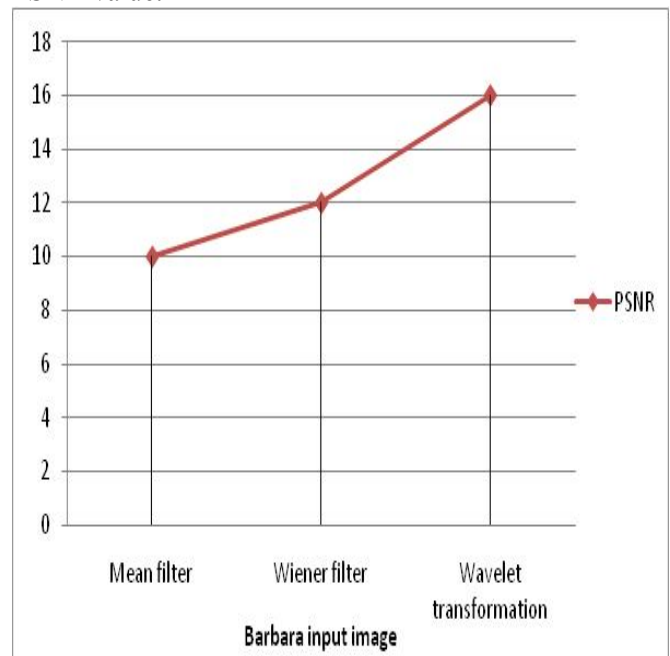


Fig 4: The above figure shows the comparative study between the image denoising techniques with barbara input image.

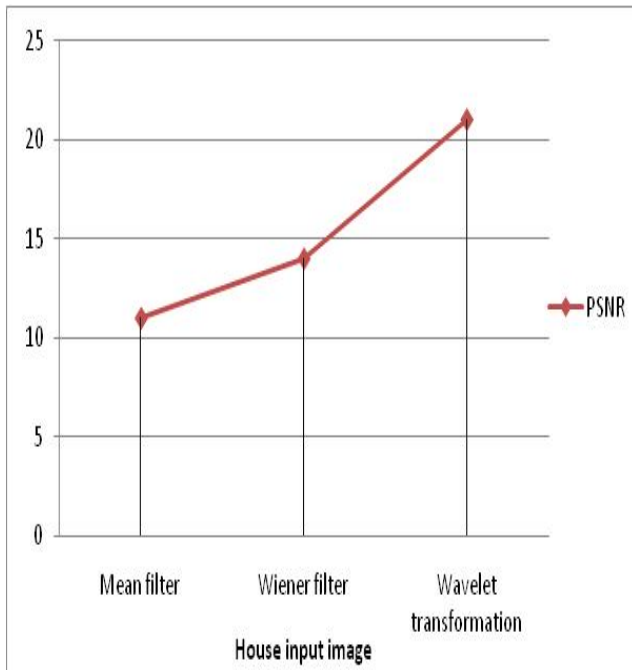


Fig 5: The above figure shows the comparative study between the image denoising techniques with house input image.

### V. Conclusion

Image de-noising finds applications in fields such as astronomy where the resolution limitations are high, in medical imaging where the physical requirements for high quality imaging are needed for analyzing the images of unique events and in the forensic science where potentially useful photographic information is sometimes of extremely bad quality. In this dissertation we present the image denoising techniques comparative performance measured with the performance parameter. This process of image denoising is done by using methods that are with like wavelet transformation, wiener filter and mean filter. This all methods implemented in MATLAB. The input images are used here for the measured of image denoising techniques comparative performance used barbara image, cameraman image and house image etc., here our present works gives better results than the existing work.

### References:

- [1] Varad A. Pimpalkhute , Rutvik Page , Ashwin Kothari, Kishor M. Bhurchandi, Vipin Milind Kamble, “Digital Image Noise Estimation Using DWT Coefficients”, IEEE transactions on image processing, 2021, pp. 1962-1972.
- [2] Hazique Aetesam, Suman Kumar Maji, Hussein Yahia, “Bayesian Approach in a Learning-Based Hyperspectral Image Denoising Framework”, IEEE Access, 2021, pp. 169335-169347.
- [3] Subrato Bharati, Tanvir Zaman Khan, Prajoy Podder , Nguyen Quoc Hung, “A comparative analysis of image denoising problem: noise models, denoising filters and applications”, 2020, pp. 1-16.
- [4] Tugba Ozge Onur, “ Improved Image Denoising Using Wavelet Edge Detection Based on Otsu's Thresholding”, Acta Polytechnica Hungarica, 2022, pp. 79-92.
- [5] Wei-Yen Hsu, Yi-Sin Chen, “Single Image Dehazing Using Wavelet-Based Haze-Lines and Denoising”, IEEE Access, 2021, pp. 104547-104559.
- [6] Chunwei Tian, Yong Xu, Wangmeng Zuo, Bo Du, Chia-Wen Lin, David Zhang, “Designing and Training of A Dual CNN for Image Denoising”, IEEE 2020, pp. 1-12.
- [7] Ozden Colak, Ender M. Eksioğlu, “On the Fly Image Denoising using Patch Ordering”, Preprint submitted to Elsevier, 2020, pp. 1-10.
- [8] Swati Rai, Jignesh S. Bhatt, S. K. Patra, “An unsupervised deep learning framework for medical image denoising”, IEEE 2020, pp. 1-22.
- [9] K. Chithra, D. Murugan, “Comparative Analysis of Image Denoising Techniques for Enhancing Real-Time Images”, International Journal of Computer



Engineering & Technology, Volume 9, 2018, pp. 250–259.

[10] Yuya Onishi, Fumio Hashimoto, Kibo Ote, Hiroyuki Ohba, Ryosuke Ota, Etsuji Yoshikawa, Yasuomi Ouchi, “Anatomical-Guided Attention Enhances Unsupervised PET Image Denoising Performance”, , pp. 1-29.

[11] Nicolo Bonettini, Carlo Andrea Gonano, Paolo Bestagini, Marco Marcon, Bruno Garavelli, Stefano Tbaro, “Multitask learning for denoising and analysis of X-ray polymer acquisitions”, IEEE 2020, pp. 1-5.

[12] Shruti Bhargava Choubey, Abhishek Choubey, Durgesh Nandan, Anurag Mahajan, “Polycystic Ovarian Syndrome Detection by Using Two-Stage Image Denoising”, Article in Traitement du Signal - August 2021, pp. 1217-1229.

[13] Yong Chen, Ting-Zhu Huang, Wei He, Xi-Le Zhao, “Hyperspectral Image Denoising Using Factor Group Sparsity-Regularized Nonconvex Low-Rank Approximation”, IEEE Transactions On Geoscience And Remote Sensing, 2021, pp. 1-16.

[14] Achleshwar Luthra, Harsh Sulakhe, Tanish Mittal, Abhishek Iyer, Santosh Yadav, “Eformer: Edge Enhancement based Transformer for Medical Image Denoising”, 2020, pp. 1-8.

[15] Bin Zhou, Biying Zhong, Jun Feng, “A Skewness Fitting Model for Noise Level Estimation and the Applications in Image Denoising”, ISAECE 2021, pp. 1-7.

[16] Kanggeun Lee, Won-Ki Jeong, “ISCL: Interdependent Self-Cooperative Learning for Unpaired Image Denoising”, IEEE Transactions On Medical Imaging, 2021, pp. 1-12.

[17] Madhu Golla, Sudipta Rudra, “A Novel Approach of K-SVD-Based Algorithm for Image Denoising”, IGI Global, 2019, pp 354-357.

[18] Rui Lai, Yiguo Mo, Zesheng Liu, Juntao Guan, “Local and Nonlocal Steering Kernel Weighted Total Variation Model for Image Denoising”, Symmetry 2019, pp 1-16.

[19] Zhenhua Gan, Fumin Zou, Nianyin Zeng, Baoping Xiong, Lyuchao Liao, Han Li, Xin Luo, Min Du, “Wavelet Denoising Algorithm Based on NDOA Compressed Sensing for Fluorescence Image of Microarray”, IEEE access, 2018, pp 13338-13346.

[20] Arundhati Misra, B Kartikeyan and S Garg “Wavelet Based SAR Data Denoising and Analysis”, IEEE, 2014, Pp 1087-1092.

[21] Yatong Xu, Xin Jin and Qionghai Dai “Spatial-temporal Depth De-noising for Kinect based on Texture Edge-assisted Depth Classification”, Digital Signal Processing, 2014, Pp 327-332.

[22] Zayed M. Ramadan “A New Method for Impulse Noise Elimination and Edge Preservation”, Electrical And Computer Engineering, 2014, Pp 2-10.

[23] Tae Hyun Kim and Kyoung Mu Lee “Segmentation-Free Dynamic Scene Deblurring”, IEEE, 2014, Pp 2766-2773.

[24] Mostafa Karbasia, Sara Bilala, Reza Aghababaeyanb, Abdolvahab Ehsani Radc, Zeeshan Bhattia and Asadullah Shaha “Analysis And Enhancement of The Denoising Depth Data Using Kinect Through Iterative Technique”, Jurnal Teknologi, 2016, Pp 185-0193.

[25] Linlin Xu, Graduate Student Jonathan Li, Yuanming Shu and Junhuan Peng “SAR Image Denoising via Clustering-Based Principal Component Analysis”, IEEE, 2014, Pp 6858-6869.

[26] Ladan Ebadi, Helmi Z. M. Shafri, Shattri B. Mansor and Ravshan Ashurov “A review of applying



second-generation wavelets for noise removal from remote sensing data”, Springer, 2013, Pp 2679-2690.

[27] Charles-Alban Deledalle, Loic Denis, Florence Tupin, Andreas Reigber and Marc Jager “NL-SAR: a unified Non-Local framework for resolution-preserving (Pol)(In)SAR denoising”, HAL, 2014, Pp 1-18.

[28] Mario Mastriani, and Alberto E. Giraldez “Neural shrinkage for wavelet-based SAR despeckling”, arxiv, 2016, Pp 1-12.

journals, conferences etc. His areas of Interests are Antenna & Wave Propagation, Digital Signal Processing, Wireless Communication, Image Processing etc.



**Aarti Gupta** received her Bachelor's degree in Electronics & communication engineering, Scope College of Engineering, Bhopal, M.P., in 2015. Currently she is pursuing Master of Technology Degree in Electronics & Communication (Digital communication) from PCST, (RGPV), Bhopal, Madhya Pradesh India. Her research area include digital image processing.



Mr. **Jitendra Mishra** he is Associate Professor and Head of the Department of Electronics and communication in PCST, Bhopal (RGPV). He received Master of Technology and Bachelor's of engineering respectively in Digital communication from BUIT, Bhopal and from RGPV, Bhopal. He has more than 12 years of teaching experience and publish 55+ papers in International